

MULTISCALE MODELING OF FLUCTUATIONS IN STOCHASTIC ELLIPTIC PDE MODELS OF NANOSENSORS

CLEMENS HEITZINGER^{†§} AND CHRISTIAN RINGHOFER^{‡¶}

Abstract. In this work, the multiscale problem of modeling fluctuations in boundary layers in stochastic elliptic partial differential equations is solved by homogenization. Homogenized equations for the covariance and variance of the solution of stochastic elliptic PDEs are derived. In addition to the homogenized equations, a scaling law for the covariance and variance as the cell size tends to zero is given. For the homogenized problems, existence and uniqueness results and a priori bounds are given and further properties are proven. The multiscale problem stems from the modeling of the electrostatics in nanoscale field-effect sensors, where the fluctuations arise from randomly distributed charge concentrations in the cells of a boundary layer. Finally, numerical results and a spectral approximation are presented.

Key words. Stochastic elliptic partial differential equation, multiscale problem, homogenization, limiting problem, scaling law, field-effect biosensor, nanowire, BioFET.

AMS subject classifications.

35B27 Homogenization; equations in media with periodic structure,
35J05 Laplacian operator, reduced wave equation (Helmholtz equation), Poisson equation,
35Q92 PDEs in connection with biology and other natural sciences,
62P30 Applications in engineering and industry,
82D80 Nanostructures and nanoparticles,
92C50 Medical applications (general).

1. Introduction. The motivation for the present study of stochastic elliptic PDE stems from the desire to model field-effect nano-sensors and hence to understand their physics. Elliptic equations, such as the Poisson equation and the linearized Poisson-Boltzmann equation, are the basic equations for their electrostatics, and the stochastic equations considered here make it possible to study fluctuations and noise in nanostructures. Furthermore, a multiscale problem is inherent in these nanoscale structures and it is solved by homogenization.

First, we introduce the physical problem. Recently, nanoscale field-effect biosensors [19–21, 24] and gas sensors [16, 22] have been demonstrated experimentally. A schematic diagram of such a sensor structure is shown in Fig. 1. The length scale of the biomolecules is in the Angstrom or nanometer range, whereas the length of the nanowire is in the micrometer range. This gives rise to a multiscale problem, since it is not possible to resolve both the boundary layer and the whole simulation domain using a single numerical grid.

This simulation problem also gives rise to a stochastic problem, since binding and unbinding events (in the case of biosensors) or chemical reactions (in the case of gas sensors) occur in the boundary layer. Additionally, the movement of the molecules in the boundary layer can be modeled by calculating their electrostatic free energy and by using a Boltzmann distribution [11]. These effects imply that the charge

[†]Department of Mathematics and Wolfgang Pauli Institute, University of Vienna, Nordbergstraße 15, A-1090 Vienna, Austria; and Department of Applied Mathematics and Theoretical Physics, University of Cambridge, Cambridge CB3 0WA, UK.

[‡]Department of Mathematics, Arizona State University, Tempe, AZ 85287, USA.

[§]This work was supported by the FWF (Austrian Science Fund) project no. P20871-N13 and by the WWTF (Viennese Science and Technology Fund) project no. MA09-028.

[¶]This work was supported by the NSF under grants DMS-0604986 and DMS-0757309.

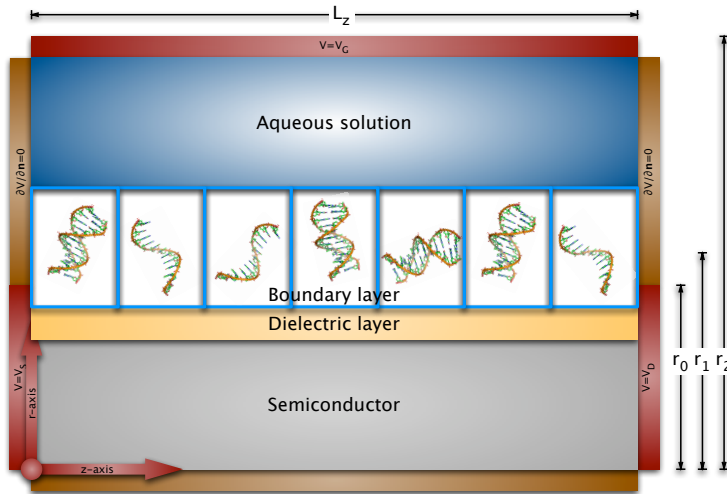


FIG. 1. Schematic diagram of a typical structure considered in this work. A nanowire field-effect sensor consists of a semiconductor nanowire with two contacts at the left and at the right, a boundary layer split into cells containing random charge distributions due to biomolecules or gas molecules, and a bulk liquid or atmosphere. Here the r - and z -axes of a cylindrical coordinate system are shown. In a DNA sensor, shown here, the immobilized probe molecules are single-stranded DNA and the target molecules are the complementary strands. After hybridization of the two strands at the sensor surface to form double-stranded DNA, the charge distribution in the biofunctionalized boundary layer is changed and hence it modulates the conductance of the semiconductor transducer. The conductance is measured between the two contacts on the left and on the right.

concentration in the boundary layer should be modeled by a random variable.

In previous work, we used deterministic PDE models and solved the multiscale problem for the deterministic Poisson equation $-\nabla \cdot (A \nabla u_\epsilon) = \rho_\epsilon$ in [12]. There, homogenization made it possible to replace the fast varying charge concentration ρ_ϵ in the boundary layer by two interface conditions for the electrostatic potential and field. The interface conditions are essentially determined by the surface charge density and the dipole moment density of the boundary layer. Of course the homogenization problem $-\nabla \cdot (A_\epsilon \nabla u_\epsilon) = \rho$ can be treated by the method of two-scale convergence resulting in a homogenized equation and a cell problem [1, 18].

In this work, we consider the stochastic Poisson equation

$$-\nabla \cdot (A(x) \nabla u_\epsilon(x, \omega)) = \rho(x, \frac{x}{\epsilon}, \omega)$$

and generalizations thereof [4, 15, 17]. Here ω is a random variable and $\epsilon \ll 1$ is ratio of the size of a cell in the boundary layer to the size of the simulation domain. The ultimate goal, when the model equation is a stochastic PDE, is to calculate the ratio

$$\frac{Eu}{\sqrt{\sigma^2 u}},$$

where u is the solution of the stochastic PDE and E and σ^2 are the expectation and variance operators with respect to ω . Hence this ratio of expectation and standard deviation is a dimensionless quantity and it is often called the signal-to-noise ratio. In engineering applications such as, e.g., field-effect sensors, the stochastic PDE is the stochastic linearized Poisson-Boltzmann equation and the signal-to-noise is to be

maximized. The results in §3 show that it is straightforward to find a deterministic PDE for the expectation Eu .

The main result of this work given in §4 is a deterministic equation for the covariance of u after homogenization. This equation immediately yields a way to calculate the variance and hence the signal-to-noise ratio. As a corollary, we also obtain a scaling law for the variance and the covariance as $\epsilon \rightarrow 0+$. The scaling law has implications for the design of field-effects sensors, since it allows to calculate noise levels.

Based on these results, an approximation of the variance and covariance of the solution is derived in §5 based on a spectral expansion [2]. The quality of the approximation is investigated in the leading example of the Laplace operator and an improvement is proposed.

This paper is organized as follows. In §2, the general operator for stochastic Poisson-type equations is introduced. In §3, a result for the expectation of weak solutions is given. In §4, the homogenization problem is defined and solved. The main result is the limiting equation for the covariance after homogenization; corollaries are given and some important properties of the limiting equations are shown. In §5, a spectral approximation for the covariance is given. Then, in §6, numerical results are presented and the spectral approximation is investigated. Finally, §7 concludes the paper.

2. The model equations. We consider linear stochastic PDE of the form

$$Lu(x, \omega) = \rho(x, \omega) \quad (1)$$

on a domain $U \subset \mathbb{R}^d$, where x is the spatial variable, ω is a random variable defined on the probability space (Ω, Σ, P) , ρ is a given function, u is the unknown, and L is a linear differential operator with respect to x . An important special case is the Poisson-Boltzmann equation

$$-\nabla \cdot (A(x)\nabla u(x)) = \rho_f(x) + \rho_m(x), \quad (2a)$$

$$\rho_m(x) := \sum_{j \in I} z_j c_j(x) q \exp(-z_j q(u(x) - \phi_F)/(k_B T)), \quad (2b)$$

where A is the permittivity, u is the electrostatic potential, ρ_f is the concentration of fixed charges, and ρ_m is the concentration of mobile charges according to a Boltzmann distribution. I is the set of charge species (ions in liquids or electrons and holes in semiconductors), $z_j \in \mathbb{Z}$ is the valence of species j , c_j is the bulk concentration of species j , q is the elementary (proton) charge, ϕ_F is the Fermi level, k_B is the Boltzmann constant, and T is the temperature. Here the bulk concentration depends on the position x meaning that only certain sub-domains are accessible by the mobile charges. For physical systems like 1:1 electrolytes and positive and negative charge carriers in semiconductors, we set $I := \{-1, +1\}$ and $z_j := j$ and we assume $c_{-1}(x) = c_1(x) =: c(x)$. This yields

$$\rho_m(x) = \sum_{k \in \{-1, +1\}} kc(x)q \exp(-kq(u(x) - \phi_F)/(k_B T)). \quad (3)$$

It is well-known that the following result holds for the semilinear Poisson-Boltzmann equation (2).

PROPOSITION 1 (Poisson-Boltzmann equation). *Suppose that the domain $U \subset \mathbb{R}^d$ is open and bounded, that A is uniformly elliptic, that $c \in \mathbb{R}^+$, that $\phi_F \in \mathbb{R}$, and that $\rho_f \in L^\infty(U)$. Then the boundary-value problem*

$$\begin{aligned} -\nabla \cdot (A\nabla u) + c(e^{(u-\phi_F)/(k_B T)} - e^{-(u-\phi_F)/(k_B T)}) - \rho_f &= 0 && \text{in } U, \\ u &= u_D && \text{on } \partial U_D, \\ \partial u / \partial n &= 0 && \text{on } \partial U_N \end{aligned}$$

has a unique solution $u \in H^1(U) \cap L^\infty(U)$. Furthermore, the estimate

$$\begin{aligned} \min \left(\inf_{\partial U_D} u_D, \phi_F + k_B T \sinh^{-1} \left(\frac{\inf_U \rho_f}{2c} \right) \right) \\ \leq u(x) \leq \max \left(\sup_{\partial U_D} u_D, \phi_F + k_B T \sinh^{-1} \left(\frac{\sup_U \rho_f}{2c} \right) \right) \end{aligned}$$

holds for all $x \in U$.

The Poisson-Boltzmann equation for arbitrary Fermi levels can be linearized as follows. Taylor expansion of (3) in ϕ around ϕ_0 yields

$$\rho_m(x) = \alpha(x) - \gamma(x)u(x) + O(u(x)^2)$$

with

$$\alpha(x) := 2c(x)q \sinh \frac{q(\phi_F - \phi_0)}{k_B T} + \frac{2c(x)q^2 \phi_0}{k_B T} \cosh \frac{q(\phi_F - \phi_0)}{k_B T}, \quad (4a)$$

$$\gamma(x) := \frac{2c(x)q^2}{k_B T} \cosh \frac{q(\phi_F - \phi_0)}{k_B T}. \quad (4b)$$

The advantage of this general form is that the expansion point ϕ_0 is not necessarily equal to the Fermi level ϕ_F [11]. Now the choice

$$Lu(x, \omega) := -\nabla \cdot (A(x)\nabla u(x, \omega)) + \gamma(x)u(x, \omega), \quad (5a)$$

$$\rho(x, \omega) := \rho_f(x, \omega) + \alpha(x) \quad (5b)$$

corresponds to the stochastic linearized Poisson-Boltzmann equation

$$-\nabla \cdot (A(x)\nabla u(x, \omega)) + \gamma(x)u(x, \omega) = \rho(x, \omega) \quad \text{in } U \times \Omega, \quad (6a)$$

$$u(x, \omega) = 0 \quad \text{on } \partial U \times \Omega \quad (6b)$$

for arbitrary Fermi levels. Much of the following pertains to general linear stochastic PDEs of the form (1), while the leading application is equation (6). Whenever further assumptions on the operator L are necessary, they include the physical situation of (4) and (6).

A variational form of (6) is to find $u \in H := H_0^1(U \times \Omega)$, H being a Hilbert space, so that $a(u, v) = \langle \rho, v \rangle$ for all $v \in H$, where a is the bilinear form

$$a(u, v) := \int_{\Omega} \int_U A(x)\nabla u(x, \omega) \cdot \nabla v(x, \omega) + \gamma(x)u(x, \omega)v(x, \omega) dx dP(\omega)$$

and $\rho \in H^{-1}$. Using this weak formulation, it is straightforward to obtain the following result.

PROPOSITION 2. *Suppose U is an open and bounded subset of \mathbb{R}^d and (Ω, Σ, P) is a probability space with bounded Ω . Suppose further that $A \in L^\infty(U, \mathbb{R}^{d \times d})$ is uniformly elliptic and that $\gamma \in L^\infty(U)$ is nonnegative. Then the boundary-value problem (6) has a unique weak solution $u \in H$ and it depends continuously on $\rho \in H^{-1}$.*

Proof. Based on the assumptions, the bilinear form $a(u, v)$ is coercive and bounded uniformly with respect to ω almost everywhere on $U \times \Omega$. Thus the existence and uniqueness of the weak solution u of (6) in H follows from the Lax-Milgram theorem and its continuous dependence on the data follows from usual estimate for $\|u\|_H$. \square

This weak formulation is an extension of the theory of deterministic elliptic equations to random fields with finite variance [3–6, 8, 14, 23]. Different choices for the Hilbert space H are possible and other theories for stochastic elliptic equations have been developed. There are also different (modeling) choices for the definition of the multiplication of random fields such as the Wick product [13].

In the following, we consider only operators L that do not depend on the random variable ω , i.e., A depends only on position. Regarding the physics of the problem, this means for Poisson-type equations that random fluctuations in the permittivity A are negligible compared to the random fluctuations in the charge distribution ρ .

3. Calculation of the expectation. We denote the expectation operator with respect to ω by E and are interested in finding an equation for the expectation Eu of the solution u of (1). Since the expectation operator E is linear, it formally commutes with the linear differential operator L , i.e., $ELu = LEu$ holds on $U \times \Omega$, and therefore the expectation Eu is the solution of the equation

$$L(Eu) = E\rho \quad \text{on } U.$$

It has the same form as the original equation (1) and the expectation $E\rho$ is known. Thus the calculation of the expectation requires the same computational effort as solving the associated deterministic equation.

In the proposition below, the formal calculation is verified for the linearized Poisson-Boltzmann equation.

LEMMA 3. *Suppose $U \subset \mathbb{R}^d$, U is open, ω is a random variable on the probability space (Ω, Σ, P) , $L = \sum_{|\alpha| \leq n} a_\alpha \partial^\alpha$ is a differential operator, and $u : U \times \Omega \rightarrow \mathbb{R}$ is measurable. Suppose further that*

$$\int_U \int_\Omega |u(x, \omega)| dP(\omega) dx < \infty \quad \text{or} \quad \int_\Omega \int_U |u(x, \omega)| dx dP(\omega) < \infty.$$

Then

$$LEu(x, \omega) = ELu(x, \omega)$$

holds on U .

Proof. It suffices to show that

$$\partial^\alpha \int_\Omega u(x, \omega) dP(\omega) = \int_\Omega \partial^\alpha u(x, \omega) dP(\omega).$$

By the definition of the weak derivative, this is equivalent to

$$\int_U \int_\Omega u(x, \omega) dP(\omega) \partial^\alpha \phi dx = (-1)^{|\alpha|} \int_U \int_\Omega \partial^\alpha u(x, \omega) dP(\omega) \phi dx \quad \forall \phi \in C_c^\infty(U),$$

which holds due to

$$(-1)^{|\alpha|} \int_U \int_\Omega \partial^\alpha u(x, \omega) dP(\omega) \phi dx = (-1)^{2|\alpha|} \int_U \int_\Omega u(x, \omega) \partial^\alpha \phi dP(\omega) dx$$

after using Fubini's theorem and partial integration. Fubini's theorem can be applied because of the assumption, because the Lebesgue measure is σ -finite, and because every probability measure is σ -finite. \square

PROPOSITION 4. *Suppose $u \in H_0^1(U \times \Omega)$ is the weak solution of the linearized Poisson-Boltzmann equation from Proposition 2. Then the expectation Eu is the unique weak solution of the deterministic boundary-value problem*

$$\begin{aligned} L(Eu) &= E\rho, \\ Eu &= 0 \quad \text{on } \partial U. \end{aligned}$$

Proof. Using the Cauchy-Schwarz inequality, we find

$$\int_\Omega \int_U |u(x, \omega)| dx dP(\omega) \leq C \|u\|_{L^2(U \times \Omega)} < \infty,$$

since $u \in L^2(U \times \Omega)$ and U and Ω are bounded. Therefore Lemma 3 can be applied. \square

4. The multiscale problem and homogenization. The multiscale problem and the boundary layer are described first. Then the main result is derived by giving a homogenization procedure. The resulting limiting equations are investigated regarding their main properties.

4.1. The boundary layer and its fine structure. We choose a Cartesian coordinate system with coordinates $x = (x_1, x_2, x_3)$ and the simulation domain U is the bounded and open subset $U := (-L_1, L_1) \times (0, L_2) \times (0, L_3) \subset \mathbb{R}^3$ (cf. Fig. 1). The boundary layer is located on the positive side of the plane $x_1 = 0$ so that x_1 is the direction normal to the surface and x_2 and x_3 are parallel to the surface. The boundary layer at $x_1 \geq 0$ is characterized by the charge concentrations $\rho(x, \omega)$ which exhibits a randomized and fast varying spatial structure. Since the fine spatial structure cannot be resolved due to computational restraints – especially in view of the stochastic nature of the problem –, the goal is to replace the original problem (6) by a homogenized problem.

We proceed by dividing the two-dimensional interface at $x_1 = 0$ into periodically repeated two-dimensional cells \mathcal{C}_k by defining

$$\mathcal{C}_k := \mathcal{C}_{(k_2, k_3)} := [\epsilon k_2, \epsilon(k_2 + 1)) \times [\epsilon k_3, \epsilon(k_3 + 1))$$

for $k = (k_2, k_3) \in \mathbb{Z} \times \mathbb{Z}$. The cells \mathcal{C}_k are of size ϵ^2 so that they cover the whole interface, i.e.,

$$[0, L_2) \times [0, L_3) \subset \bigcup_{\substack{1 \leq k_2 \leq K_2 \\ 1 \leq k_3 \leq K_3}} \mathcal{C}_k$$

holds with $K_2 := \lceil L_2/\epsilon \rceil$ and $K_3 := \lceil L_3/\epsilon \rceil$. We use multi-indices $k = (k_2, k_3)$ with $k_2 \in \{0, \dots, K_2 - 1\}$ and $k_3 \in \{0, \dots, K_3 - 1\}$ for the cells \mathcal{C}_k , and we denote the

total number of cells in the boundary layer by $K := K_2 K_3$ and the index set of the cell indices by $\mathcal{K} := \{(0, 0), \dots, (K_2 - 1, K_3 - 1)\}$ so that $|\mathcal{K}| = K$.

Three-dimensional cells are denoted by $[0, L_1] \times \mathcal{C}_k$. The positive real number $\epsilon \ll 1$ denotes the ratio of the cell size to the whole simulation domain U . We use a homogenization ansatz where we scale the boundary layer by introducing fast variables. We stretch the x_1 -, x_2 -, and x_3 -coordinates at the interface $x_1 = 0$ by a factor of $1/\epsilon$ and hence obtain the fast variables x_1/ϵ , x_2/ϵ , and x_3/ϵ in contrast to the slow variables x_1 , x_2 , and x_3 . The idea of the multiscale ansatz is to write the function $\rho(x_1, x_2, x_3)$ as a function $\hat{\rho}$ of both the fast and the slow variables, i.e.,

$$\rho(x_1, x_2, x_3) = \hat{\rho}\left(\frac{x_1}{\epsilon}, \frac{x_2}{\epsilon}, \frac{x_3}{\epsilon}, x_2, x_3\right). \quad (7)$$

The dependence on x_2 and x_3 includes slow variations in $\hat{\rho}$ in the boundary layer. The function $\hat{\rho}(x_1/\epsilon, x_2/\epsilon, x_3/\epsilon, x_2, x_3)$ is quasi-periodic: it is 1-periodic in the second argument x_2/ϵ and in the third argument x_3/ϵ , i.e.,

$$\hat{\rho}\left(\frac{x_1}{\epsilon}, \frac{x_2}{\epsilon}, \frac{x_3}{\epsilon}, x_2, x_3\right) = \hat{\rho}\left(\frac{x_1}{\epsilon}, \frac{x_2}{\epsilon} + k_2, \frac{x_3}{\epsilon} + k_3, x_2, x_3\right)$$

holds for all integers k_2 and k_3 . This is consistent with the definition of the cells \mathcal{C}_k . Furthermore $\hat{\rho}$ decays to zero sufficiently fast as $x_1 \rightarrow \infty$, i.e., the charges in the boundary layer are concentrated close to the interface at $x_1 = 0$. These considerations motivate the following definition.

DEFINITION 5 (boundary-layer function). *Suppose $U \subset \mathbb{R}^3$. A function $\rho \in L^2(U)$ is called a boundary-layer function if it can be written in the form*

$$\rho(x_1, x_2, x_3) = \hat{\rho}\left(\frac{x_1}{\epsilon}, \frac{x_2}{\epsilon}, \frac{x_3}{\epsilon}, x_2, x_3\right),$$

where $\hat{\rho}$ is 1-periodic in its second and third arguments and $\lim_{x_1 \rightarrow \infty} \rho(x_1, x_2, x_3) = 0$ holds.

We now describe the charge concentration $\rho(x, \omega)$ in the boundary layer more precisely in terms of the random variable. For each cell \mathcal{C}_k , there is a random variable ω_k so that the charge concentration ρ_k of cell \mathcal{C}_k depends on ω_k . In reality, the different states of the random variable ω_k correspond to the presence of different molecules and to different orientations thereof the boundary layer. We define the random variable

$$\omega := (\omega_1, \dots, \omega_K)$$

that includes the states of all cells in the boundary layer. Using these definitions, we write the charge concentration ρ of the whole boundary layer as

$$\rho(x, \omega) = \sum_{k \in \mathcal{K}} \chi_k(x) \rho_k(x, \omega_k),$$

where $\chi_k(x) = \chi_k(x_2, x_3)$ is the characteristic function of the cell \mathcal{C}_k , i.e., it equals 1 if $(x_2, x_3) \in \mathcal{C}_k$ and 0 otherwise.

4.2. Homogenization and the theorem for the limiting equation. We start the homogenization procedure with some definitions.

DEFINITION 6 (centered random variable). *Let X be a random variable. Then $\tilde{X} := X - EX$ is called the corresponding centered random variable.*

DEFINITION 7 (joint moment). *Suppose α is a multi-index of dimension $J := \dim \alpha$. The joint moment M_α of the J random variables X_j is defined as*

$$M_\alpha(X_1, \dots, X_J) := E \left(\prod_{j=1}^J (X_j - EX_j)^{\alpha_j} \right).$$

To simplify the calculations, we will use the centered potential \tilde{u} and the centered charge concentrations $\tilde{\rho}_k$ and $\tilde{\rho}$. For the centered quantities, the identities $E\tilde{u} = 0$, $E\tilde{\rho} = 0$, $E\tilde{\rho}_k = 0$, and

$$\tilde{\rho}(x, \omega) = \sum_{k \in \mathcal{K}} \chi_k(x) \tilde{\rho}_k(x, \omega_k) \quad (8)$$

hold and we immediately find

$$L\tilde{u} = \tilde{\rho}. \quad (9)$$

The covariance of two random variables X_1 and X_2 is defined as $\text{cov}(X_1, X_2) := M_{(1,1)}(X_1, X_2)$. To simplify notation, we write

$$(\text{cov } u)(x, y) := \text{cov}(u(x, \cdot), u(y, \cdot))$$

for the covariance of u evaluated at x and $y \in U$, and we denote the variance of u calculated at $x \in U$ by

$$(\sigma^2 u)(x) := (\text{cov } u)(x, x).$$

Of course the equations $\text{cov } u = \text{cov } \tilde{u}$ and $\sigma^2 u = \sigma^2 \tilde{u}$ holds for the centered covariance and variance.

Suppose that G is a Green's function of L on U , i.e.,

$$LG(x, y) = \delta(x - y) \quad \forall x, y \in U$$

holds. Note that L and therefore G are independent of ϵ . Using the Green's function G , the solution \tilde{u} of (9) is given by

$$\tilde{u}(x, \omega) = \int_U G(x, y) \tilde{\rho}(y, \omega) dy.$$

To calculate the joint moments of $X_j := \tilde{u}(x_j, \omega)$, we first write the integrand as

$$\prod_{j=1}^J \tilde{u}(x_j, \omega)^{\alpha_j} = \int_{U^{|\alpha|}} \prod_{j=1}^J \prod_{\nu=1}^{\alpha_j} (G(x_j, \xi_{j\nu}) \tilde{\rho}(\xi_{j\nu}, \omega)) d\xi_{11} \dots \xi_{1\alpha_1} \dots \xi_{J1} \dots \xi_{J\alpha_J},$$

where $|\alpha| = \sum_{j=1}^J \alpha_j$, and use (8) to find

$$\begin{aligned} M_\alpha(\tilde{u}(x_j, \omega)) &= \int_\Omega \prod_{j=1}^J \tilde{u}(x_j, \omega)^{\alpha_j} dP(\omega) \\ &= \int_\Omega \int_{U^{|\alpha|}} \prod_{j=1}^J \prod_{\nu=1}^{\alpha_j} (G(x_j, \xi_{j\nu}) \sum_{k_{j\nu} \in \mathcal{K}} \chi_{k_{j\nu}}(\xi_{j\nu}) \tilde{\rho}_{k_{j\nu}}(\xi_{j\nu}, \omega_{k_{j\nu}})) d\xi_{11} \dots \xi_{J\alpha_J} dP(\omega). \end{aligned}$$

We denote the characteristic function of the interval $[0, 1)$ by χ and hence we have

$$\chi_k(x) = \chi_{(k_2, k_3)}(x_2, x_3) = \chi\left(\frac{x_2}{\epsilon} - k_2\right) \chi\left(\frac{x_3}{\epsilon} - k_3\right)$$

for the characteristic function χ_k of cell \mathcal{C}_k . Now the moment M_α is given by

$$\begin{aligned} M_\alpha(\tilde{u}(x_j, \omega)) &= \int_\Omega \int_{U^{|\alpha|}} \left(\prod_{j=1}^J \prod_{\nu=1}^{\alpha_j} G(x_j, \xi_{j\nu}) \right) \\ &\cdot \sum_{k_{11} \in \mathcal{K}} \cdots \sum_{k_{J\alpha_J} \in \mathcal{K}} \chi_{k_{11}}(\xi_{11}) \cdots \chi_{k_{J\alpha_J}}(\xi_{J\alpha_J}) \tilde{\rho}_{k_{11}}(\xi_{11}, \omega_{k_{11}}) \cdots \tilde{\rho}_{k_{J\alpha_J}}(\xi_{J\alpha_J}, \omega_{k_{J\alpha_J}}) \\ &\quad d\xi_{11} \dots \xi_{J\alpha_J} dP(\omega) \\ &= \sum_{k_{11} \in \mathcal{K}} \cdots \sum_{k_{J\alpha_J} \in \mathcal{K}} \int_\Omega \int_0^\infty \int_{\epsilon k_{11,2}}^{\epsilon(k_{11,2}+1)} \int_{\epsilon k_{11,3}}^{\epsilon(k_{11,3}+1)} \cdots \\ &\quad \cdots \int_0^\infty \int_{\epsilon k_{J\alpha_J,2}}^{\epsilon(k_{J\alpha_J,2}+1)} \int_{\epsilon k_{J\alpha_J,3}}^{\epsilon(k_{J\alpha_J,3}+1)} \\ &\quad \left(\prod_{j=1}^J \prod_{\nu=1}^{\alpha_j} G(x_j, \xi_{j\nu}) \right) \tilde{\rho}_{k_{11}}(\xi_{11}, \omega_{k_{11}}) \cdots \tilde{\rho}_{k_{J\alpha_J}}(\xi_{J\alpha_J}, \omega_{k_{J\alpha_J}}) \\ &\quad d\xi_{J\alpha_J,3} \xi_{J\alpha_J,2} \xi_{J\alpha_J,1} \cdots \xi_{11,3} \xi_{11,2} \xi_{11,1} dP(\omega). \end{aligned}$$

We use the multiscale ansatz for the boundary-layer function $\tilde{\rho}_k$ so that

$$\begin{aligned} \tilde{\rho}_k(x, \omega_k) &= \hat{\rho}_k\left(\frac{x_1}{\epsilon}, \frac{x_2}{\epsilon} - k_2, \frac{x_3}{\epsilon} - k_3, \omega_k\right) \\ &= \hat{\rho}\left(\frac{x_1}{\epsilon}, \frac{x_2}{\epsilon} - k_2, \frac{x_3}{\epsilon} - k_3, \epsilon k_2, \epsilon k_3, \omega_k\right). \end{aligned}$$

The function $\hat{\rho}_k$ depends on the cell index k , whereas $\hat{\rho}$ depends on the slow variables $x_2 = \epsilon k_2$ and $x_3 = \epsilon k_3$ instead of the cell index. To simplify notation, we write $\tilde{\rho}_k$ again for $\hat{\rho}_k$.

For the moment M_α , this yields

$$\begin{aligned} M_\alpha(\tilde{u}(x_j, \omega)) &= \sum_{k_{11} \in \mathcal{K}} \cdots \sum_{k_{J\alpha_J} \in \mathcal{K}} \int_\Omega \int_0^\infty \int_{\epsilon k_{11,2}}^{\epsilon(k_{11,2}+1)} \int_{\epsilon k_{11,3}}^{\epsilon(k_{11,3}+1)} \cdots \\ &\quad \cdots \int_0^\infty \int_{\epsilon k_{J\alpha_J,2}}^{\epsilon(k_{J\alpha_J,2}+1)} \int_{\epsilon k_{J\alpha_J,3}}^{\epsilon(k_{J\alpha_J,3}+1)} \left(\prod_{j=1}^J \prod_{\nu=1}^{\alpha_j} G(x_j, \xi_{j\nu}) \right) \\ &\cdot \tilde{\rho}_{k_{11}}\left(\frac{\xi_{11,1}}{\epsilon}, \frac{\xi_{11,2}}{\epsilon} - k_2, \frac{\xi_{11,3}}{\epsilon} - k_3, \omega_{k_{11}}\right) \cdots \tilde{\rho}_{k_{J\alpha_J}}\left(\frac{\xi_{J\alpha_J,1}}{\epsilon}, \frac{\xi_{J\alpha_J,2}}{\epsilon} - k_2, \frac{\xi_{J\alpha_J,3}}{\epsilon} - k_3, \omega_{k_{J\alpha_J}}\right) \\ &\quad d\xi_{J\alpha_J,3} \xi_{J\alpha_J,2} \xi_{J\alpha_J,1} \cdots \xi_{11,3} \xi_{11,2} \xi_{11,1} dP(\omega). \end{aligned}$$

After substituting

$$\begin{aligned} \bar{\xi}_{j\nu,1} &:= \frac{1}{\epsilon} \xi_{j\nu,1}, \\ \bar{\xi}_{j\nu,2} &:= \frac{1}{\epsilon} \xi_{j\nu,2} - k_{j\nu,2}, \\ \bar{\xi}_{j\nu,3} &:= \frac{1}{\epsilon} \xi_{j\nu,3} - k_{j\nu,3} \end{aligned}$$

and renaming, we find

$$\begin{aligned}
M_\alpha(\tilde{u}(x_j, \omega)) &= \epsilon^{3|\alpha|} \sum_{k_{11} \in \mathcal{K}} \dots \sum_{k_{J\alpha_J} \in \mathcal{K}} \int_{\Omega} \int_0^\infty \int_0^1 \int_0^1 \dots \int_0^\infty \int_0^1 \int_0^1 \\
&\quad \left(\prod_{j=1}^J \prod_{\nu=1}^{\alpha_j} G(x_j, (\epsilon \xi_{j\nu,1}, \epsilon(\xi_{j\nu,2} + k_{j\nu,2}), \epsilon(\xi_{j\nu,3} + k_{j\nu,3}))) \right) \cdot \\
&\quad \cdot \tilde{\rho}_{k_{11}}(\xi_{11}, \omega_{k_{11}}) \dots \tilde{\rho}_{k_{J\alpha_J}}(\xi_{J\alpha_J}, \omega_{k_{J\alpha_J}}) \\
&\quad d\xi_{J\alpha_J,3} \xi_{J\alpha_J,2} \xi_{J\alpha_J,1} \dots \xi_{11,3} \xi_{11,2} \xi_{11,1} dP(\omega).
\end{aligned}$$

The product involving the Green's function G on the right-hand side can be simplified by noting that L and hence G do not depend on ϵ (apart from the arguments above) and by supposing that G is smooth enough, which is the case at least when L is a Laplace-type operator. Since $\xi_{j\nu,i} \in [0, 1]$, $\epsilon \xi_{j\nu,i} = O(\epsilon)$ holds for all $i \in \{1, \dots, d\}$. Furthermore, $k_{j\nu,i} = O(1/\epsilon)$ holds for $i \in \{2, 3\}$ by the definition of K_i and therefore $\epsilon k_{j\nu,i} = O(1)$. Hence Taylor expansion of the Green's function G yields

$$\begin{aligned}
&G(x_j, (\epsilon \xi_{j\nu,1}, \epsilon(\xi_{j\nu,2} + k_{j\nu,2}), \epsilon(\xi_{j\nu,3} + k_{j\nu,3}))) \\
&= G(x_j, (0, \epsilon k_{j\nu,2}, \epsilon k_{j\nu,3})) + \epsilon \xi_{j\nu} \cdot \nabla_2 G(x_j, (0, \epsilon k_{j\nu,2}, \epsilon k_{j\nu,3})) + O(\epsilon^2).
\end{aligned}$$

After dropping terms of order ϵ and higher, we therefore obtain

$$\begin{aligned}
M_\alpha(\tilde{u}(x_j, \omega)) &= \epsilon^{3|\alpha|} \sum_{k_{11} \in \mathcal{K}} \dots \sum_{k_{J\alpha_J} \in \mathcal{K}} \int_{\Omega} \int_0^\infty \int_0^1 \int_0^1 \dots \int_0^\infty \int_0^1 \int_0^1 \\
&\quad \left(\prod_{j=1}^J \prod_{\nu=1}^{\alpha_j} G(x_j, (0, \epsilon k_{j\nu,2}, \epsilon k_{j\nu,3})) \right) \tilde{\rho}_{k_{11}}(\xi_{11}, \omega_{k_{11}}) \dots \tilde{\rho}_{k_{J\alpha_J}}(\xi_{J\alpha_J}, \omega_{k_{J\alpha_J}}) \\
&\quad d\xi_{J\alpha_J,3} \xi_{J\alpha_J,2} \xi_{J\alpha_J,1} \dots \xi_{11,3} \xi_{11,2} \xi_{11,1} dP(\omega)
\end{aligned}$$

and further

$$\begin{aligned}
M_\alpha(\tilde{u}(x_j, \omega)) &= \epsilon^{3|\alpha|} \sum_{k_{11} \in \mathcal{K}} \dots \sum_{k_{J\alpha_J} \in \mathcal{K}} \prod_{j=1}^J \prod_{\nu=1}^{\alpha_j} G(x_j, (0, \epsilon k_{j\nu,2}, \epsilon k_{j\nu,3})) \cdot \\
&\quad \cdot \int_0^\infty \int_0^1 \int_0^1 \dots \int_0^\infty \int_0^1 \int_0^1 M_\alpha(\tilde{\rho}_{k_{11}}, \dots, \tilde{\rho}_{k_{J\alpha_J}}) d\xi_{J\alpha_J} \dots \xi_{11}.
\end{aligned}$$

This is a general representation of the joint moment $M_\alpha(\tilde{u}(x_j, \omega))$ of $\tilde{u}(x_j, \omega)$ in terms of the joint moment $M_\alpha(\tilde{\rho}_{k_{j\nu}})$ of the data ρ .

To obtain specific results for the covariance $M_{(1,1)}$ and then for the variance $M_{(2)}$, we assume that the molecules in each cell do not affect the molecules in the other cells. This assumption is satisfied in realistic structures, since their distance is large enough to ensure full electrostatic screening, and it is well supported by our Monte-Carlo simulations of screening [7]. Thus we assume that $\tilde{\rho}_k$ and $\tilde{\rho}_\ell$ are independent for $k \neq \ell$ and hence uncorrelated. This means

$$k \neq \ell \implies \text{cov}(\tilde{\rho}_k(y, \cdot), \tilde{\rho}_\ell(z, \cdot)) = 0 \quad \forall y, z \in U, \quad \forall k, \ell \in \mathcal{K},$$

which implies

$$\int_{\Omega} \tilde{\rho}_k(y, \omega_k) \tilde{\rho}_\ell(z, \omega_\ell) dP(\omega) = \delta_{k\ell} \int_{\Omega} \tilde{\rho}_k(y, \omega_k) \tilde{\rho}_k(z, \omega_k) dP(\omega) \quad \forall y, z \in U,$$

where $\delta_{k\ell}$ is the Kronecker delta. Using this last equation and the definition

$$R(k, \omega_k) := \int_0^\infty \int_0^1 \int_0^1 \tilde{\rho}_k(x_1, x_2, x_3, \omega_k) dx_3 x_2 x_1, \quad (10)$$

the covariance simplifies to

$$\begin{aligned} (\text{cov } u)(y, z) &= M_{(1,1)}(\tilde{u}(y, \omega), \tilde{u}(z, \omega)) \\ &= \epsilon^6 \sum_{k \in \mathcal{K}} \sum_{\ell \in \mathcal{K}} G(y, (0, \epsilon k_2, \epsilon k_3)) G(z, (0, \epsilon \ell_2, \epsilon \ell_3)) \cdot \\ &\quad \cdot \int_0^\infty \int_0^1 \int_0^1 \int_0^\infty \int_0^1 \int_0^1 \int_{\Omega} \tilde{\rho}_k(y, \omega_k) \tilde{\rho}_\ell(z, \omega_\ell) dP(\omega) dz_3 z_2 z_1 y_3 y_2 y_1 \\ &= \epsilon^6 \sum_{k \in \mathcal{K}} G(y, (0, \epsilon k_2, \epsilon k_3)) G(z, (0, \epsilon k_2, \epsilon k_3)) \cdot \\ &\quad \cdot \int_0^\infty \int_0^1 \int_0^1 \int_0^\infty \int_0^1 \int_0^1 \int_{\Omega} \tilde{\rho}_k(y, \omega_k) \tilde{\rho}_k(z, \omega_k) dP(\omega) dz_3 z_2 z_1 y_3 y_2 y_1 \\ &= \epsilon^6 \sum_{k \in \mathcal{K}} G(y, (0, \epsilon k_2, \epsilon k_3)) G(z, (0, \epsilon k_2, \epsilon k_3)) \int_{\Omega} R(k, \omega_k)^2 dP(\omega_k). \end{aligned}$$

We define

$$\bar{R}(\epsilon k_2, \epsilon k_3) := \left(\int_{\Omega} R(k, \omega_k)^2 dP(\omega_k) \right)^{1/2} \quad (11)$$

and convert the Riemann sum over k_2 and k_3 into a two-dimensional integral over y_2 and y_3 to find

$$(\text{cov } u)(y, z) \approx \epsilon^4 \int_0^{L_3} \int_0^{L_2} G(y, (0, x_2, x_3)) G(z, (0, x_2, x_3)) \bar{R}(x_2, x_3)^2 dx_2 x_3. \quad (12)$$

Here \bar{R} is evaluated at the point (x_2, x_3) that lies in cell $k = (k_2, k_3)$ determined by the equations $x_2 = \epsilon k_2$ and $x_3 = \epsilon k_3$.

Finally, we apply L_y , i.e., the operator L with derivatives with respect to y , to find

$$\begin{aligned} L_y(\text{cov } u)(y, z) &= \epsilon^4 \int_0^{L_3} \int_0^{L_2} \delta(y_1, y_2 - x_2, y_3 - x_3) G(z, (0, x_2, x_3)) \bar{R}(x_2, x_3)^2 dx_2 x_3, \end{aligned}$$

and we apply L_z , the operator with respect to z , to find

$$\begin{aligned} L_z L_y(\text{cov } u)(y, z) &= \epsilon^4 \int_0^{L_3} \int_0^{L_2} \delta(y_1, y_2 - x_2, y_3 - x_3) \delta(z_1, z_2 - x_2, z_3 - x_3) \bar{R}(x_2, x_3)^2 dx_2 x_3 \\ &= \epsilon^4 \delta(y_1, z_1, y_2 - z_2, y_3 - z_3) \bar{R}(y_2, y_3)^2. \end{aligned}$$

In summary, we have (formally) proved the following result.

THEOREM 8 (limiting problem for the covariance). *Let ρ_k be boundary-layer functions on U and L be a differential operator independent of ϵ with a smooth Green's function G . Then the limiting problem for $\epsilon \rightarrow 0+$ for the covariance $\text{cov } u$ of the solution u of the boundary-value problem*

$$Lu(x, \omega) = \rho(x, \omega)$$

is the boundary-value problem

$$L_z L_y (\text{cov } u)(y, z) = \epsilon^4 \delta(y_1, z_1, y_2 - z_2, y_3 - z_3) \bar{R}(y_2, y_3)^2, \quad (13)$$

where \bar{R} is given by (11) and (10).

Note that due to the delta distributions on the right-hand side, the equation is symmetric in y and z .

COROLLARY 9 (limiting problem for the variance). *Under the assumptions of Theorem 8, the limiting problem for $\epsilon \rightarrow 0+$ for the variance $\sigma^2 u$ of the solution u of the boundary-value problem $Lu(x, \omega) = \rho(x, \omega)$ is the boundary-value problem*

$$L_x^2 (\sigma^2 u)(x) = \epsilon^4 \delta(x_1) \bar{R}(x_2, x_3)^2.$$

Note that due to the factors $\delta(y_1, z_1)$ and $\delta(x_1)$ on the right-hand sides, the covariance and the variance are concentrated at the interface $x_1 = 0$. Regarding the physics of the problem, R can be interpreted as the surface charge density of the boundary layer as a function of the slow variables for a given value of ω_k . Then \bar{R}^2 is the variance (with respect to the random variable ω_k) of the surface charge density R .

Equation (12) in the proof yields the following scaling law.

COROLLARY 10 (scaling law for the variance and covariance). *Under the assumptions of Theorem 8, the variance $\sigma^2 \tilde{u} = \sigma^2 u$ and the covariance $\text{cov } \tilde{u} = \text{cov } u$ scale like ϵ^4 as $\epsilon \rightarrow 0$.*

4.3. Existence, uniqueness, and further properties. Having found the limiting problems, the properties of their solutions are investigated here. It is expected that their solutions, being interpreted as covariances or variances, are unique. A priori bounds are also given. Furthermore, it is expected that the variance is nonnegative and the covariance is symmetric.

We start by showing the existence and uniqueness of the solution of the limiting equation for the variance given in Corollary 9. Suppose that L is an elliptic operator in divergence form, i.e.,

$$Lu := -\nabla \cdot (A \nabla u) + b \cdot \nabla u + cu.$$

This form includes, of course, the linearized Poisson-Boltzmann equation, i.e., the case where L is given by (5a) and (4). Because of Corollary 9, we consider equations of the form $L^2 u = f$ such that the unknown u is the variance. Partial integration yields that

$$\int_U (L^2 u) v dx = a_2(u, v)$$

holds for all $u, v \in H_0^2(U) := \{w \in H^2(U) \mid w = 0 = (A^\top \nabla w) \cdot \mathbf{n} \text{ on } \partial U\}$, where we have defined the bilinear form a_2 as

$$a_2(u, v) := \int_U (Lu)(L^* v) dx$$

and

$$L^*v = -\nabla \cdot (A^\top \nabla v) - \nabla \cdot (bv) + cv$$

is the adjoint of L . Hence the weak formulation of $L^2u = f$ is to find $u \in H_0^2(U)$ so that

$$a_2(u, v) = \langle f, v \rangle \quad \forall v \in H_0^2(U),$$

where $f \in H^{-2}(U)$.

To show that the bilinear form a_2 is coercive, we will need the following lemma.

LEMMA 11. *Suppose U is a bounded, open subset of \mathbb{R}^d with a C^2 boundary and suppose that*

$$Lu := -\nabla \cdot (A\nabla u) + b \cdot \nabla u + cu$$

is a differential operator, where $A \in C^1(\bar{U}, \mathbb{R}^{d \times d})$ is uniformly elliptic with ellipticity constant θ , $b \in L^\infty(U, \mathbb{R}^d)$, and $c \in L^\infty(U, \mathbb{R})$. Suppose further that $b = 0$ and $c \geq 0$ for all $x \in U$ or that $\|b\|_{L^\infty}^2 \leq 4\theta \inf_{x \in U} c$ holds. Then

$$u \mapsto \|u\|_{H^2(U)} \quad \text{and} \quad u \mapsto \|Lu\|_{L^2(U)}$$

are equivalent norms on $H^2(U) \cap H_0^1(U)$.

For completeness, the proof is given in Appendix A.

PROPOSITION 12. *Suppose U is a bounded, open subset of \mathbb{R}^d with a C^2 boundary and suppose that*

$$Lu := -\nabla \cdot (A\nabla u) + cu$$

is a differential operator, where $A \in C^1(\bar{U}, \mathbb{R}^{d \times d})$ is symmetric and uniformly elliptic and $c \in L^\infty(U, \mathbb{R})$ is nonnegative for all $x \in U$. Then the boundary-value problem

$$\begin{aligned} L^2u &= f & \text{in } U, \\ u &= 0 & \text{on } \partial U, \\ \frac{\partial u}{\partial n} &= 0 & \text{on } \partial U \end{aligned}$$

has a unique weak solution $u \in H_0^2(U)$ and there is a constant C such that the estimate

$$\|u\|_{H^2(U)} \leq C \|f\|_{H^{-2}(U)}$$

holds.

Proof. The operator L is self-adjoint due to $A = A^\top$. First, we show that a_2 is continuous, i.e., there is a constant C so that $|a_2(u, v)| \leq C \|u\|_{H^2(U)} \|v\|_{H^2(U)}$. The corresponding estimate

$$\begin{aligned} |a_2(u, v)| &= \left| \int_U (Lu)(L^*v) dx \right| \leq \int_U |Lu||L^*v| dx \\ &\leq \|Lu\|_{L^2(U)} \|L^*v\|_{L^2(U)} \leq C \|u\|_{H^2(U)} \|v\|_{H^2(U)} \end{aligned}$$

follows from the Cauchy-Schwarz inequality and Lemma 11.

Second, we show that a_2 is coercive. Since L is self-adjoint, we find

$$a_2(u, u) = \int_U (Lu)(L^*u)dx = \int_U (Lu)^2dx = \|Lu\|_{L^2(U)}^2 \geq C\|u\|_{H^2(U)}^2$$

due to Lemma 11.

Using the Lax-Milgram theorem now yields the existence and uniqueness of the solution as well as the estimate. \square

This proposition implies that the limiting problem for the variance given in Corollary 9 has a unique solution σ^2u . Since the solution σ^2u is interpreted as a variance, the question arises if we can show that the solution of the limiting problem is always nonnegative. Under an additional assumption motivated by the physics of the problem, a positive answer is given by the following proposition. This assumption is that far enough away from the finite support of $\rho(x, \omega)$, the variance σ^2u and its derivatives vanish since there is no uncertainty, i.e., $L(\sigma^2u)$ vanishes.

PROPOSITION 13. *Suppose that $v := \sigma^2u \in H_0^2(U)$ is the unique solution of the limiting problem as in Corollary 9 and Proposition 12. Suppose further that $Lv \geq 0$ on ∂U . Then $v \geq 0$ in \bar{U} .*

Proof. We apply the weak maximum principle for elliptic equations to the limiting problem

$$L^2v = Lw = \epsilon^4\delta(x_1)\bar{R}(x_2, x_3)^2 \geq 0,$$

where $w := Lv$, to conclude that $w \geq 0$ in \bar{U} due to $w \geq 0$ on ∂U . Since $Lv \geq 0$ and $v = 0$ on ∂U , we use the maximum principle again to conclude that $v \geq 0$ as claimed. \square

Since the covariance is by definition symmetric in its two arguments, it is expected that symmetry is preserved by homogenization, i.e., that the solution $\text{cov } u$ of the homogenized equation (13) in Theorem 8 is symmetric in y and z . This is indeed the case due to the following proposition. For notational simplicity we write u for $\text{cov } u$.

PROPOSITION 14. *Suppose that the boundary conditions of the boundary-value problem $L_zL_yu(y, z) = f(y, z)$ and the right-hand side f are symmetric in y and z and that u is a weak solution of this problem. Then u is symmetric a.e.*

Proof. We denote the symmetric part of $u(y, z)$ by $v(y, z) := (u(y, z) + u(z, y))/2$ and its antisymmetric part by $w(y, z) := (u(y, z) - u(z, y))/2$. The weak formulation of the problem is

$$\iint L_yu(y, z)L_z^*\phi(y, z) - f(y, z)\phi(y, z)dyz = 0 \quad (14)$$

for all test functions ϕ . Interchanging y and z yields

$$\iint L_zu(z, y)L_y^*\phi(z, y) - f(z, y)\phi(z, y)dyz = 0$$

and swapping L_y and L_z using their adjoints, using the symmetry of f , and replacing $\phi(z, y)$ by $\phi(y, z)$ (since the equation holds for all test functions) yields

$$\iint L_yu(z, y)L_z^*\phi(y, z) - f(y, z)\phi(y, z)dyz = 0. \quad (15)$$

Finally subtracting (15) from (14) yields $\iint L_yw(y, z)L_z^*\phi(y, z)dyz = 0$ and hence

$$\iint w(y, z)L_y^*L_z^*\phi(y, z)dyz = 0$$

holds for all test functions ϕ . Therefore the antisymmetric part w vanishes a.e. \square

PROPOSITION 15. *Suppose that $U \subset \mathbb{R}^d$ is a bounded domain and that ∂U is C^2 , suppose that $f \in L^2(U \times U)$, and suppose that $L_x = -\nabla_x \cdot (A(x)\nabla_x)$ is an elliptic operator with $a_{ij} \in C^1(\bar{U})$ and that A is uniformly elliptic with constant α . Then the boundary-value problem*

$$L_z L_y u(y, z) = f(y, z)$$

on $D \times D$ with homogeneous Dirichlet boundary conditions has a unique solution $u \in H^1(U \times U)$ and the estimate

$$\|u\|_{H^1(U \times U)} \leq \frac{\sqrt{2}}{\alpha^2} \|f\|_{L^2(U \times U)}$$

holds.

Proof. We use the Lax-Milgram theorem twice. First, we consider the boundary-value problem $L_z w(y, z) = f(y, z)$ for all $y \in U$. It has a unique solution $w(y, \cdot) \in H^2(U)$ for all $y \in U$, since $f \in L^2(U \times U)$, and the inequality $\|w\|_{L^2(U \times U)} \leq \alpha^{-1} \|f\|_{L^2(U \times U)}$ follows immediately.

Second, we consider the boundary-value problem $L_y u(y, z) = w(y, z)$ for all $z \in U$. It has a unique solution $u(\cdot, z) \in H^2(U)$ for all $z \in U$ and the usual estimate $\|u(\cdot, z)\|_{H^2(U)} \leq \alpha^{-1} \|w(\cdot, z)\|_{L^2(U)}$ holds for all $z \in U$.

The problem $L_y L_z u(y, z) = f(y, z)$ is equivalent to the original problem; we can use the definition of the weak derivative and Fubini's theorem to show that L_y and L_z can be interchanged as in the proof of Lemma 3, since an iterated integral converges. This yields the symmetric estimate $\|u(y, \cdot)\|_{H^2(U)} \leq \alpha^{-1} \|w(y, \cdot)\|_{L^2(U)}$ for all $y \in U$.

Finally, the last two estimates yield the asserted estimate. \square

5. Spectral approximation of the covariance and variance. The main idea of the spectral approximation given here is to approximate the covariance or variance by using only the most significant of the eigenvalues and eigenfunctions of G . This eigensystem of G can be calculated using the well-known numerical procedures from a discretization of L .

PROPOSITION 16. *Suppose that U is an open, bounded, and connected subset of \mathbb{R}^d and that the differential operator L has the divergence form*

$$Lu := -\nabla \cdot (A\nabla u) + cu,$$

where A is uniformly elliptic and symmetric and the coefficients A and c are bounded. Then the covariance $\text{cov } u$ in Theorem 8 is given by

$$(\text{cov } u)(y, z) = \sum_{j=1}^{\infty} \sum_{k=1}^{\infty} \lambda_j \lambda_k \psi_j(y) \psi_k(z) T_{jk}, \quad (16)$$

where $\{\lambda_n\}$ and $\{\psi_n\}$ are the eigenvalues and eigenfunctions of the Green's function of the operator L and the coefficients T_{jk} are defined as

$$T_{jk} := \epsilon^4 \int_0^{L_3} \int_0^{L_2} \psi_j(0, \eta_2, \eta_3) \psi_k(0, \eta_2, \eta_3) \bar{R}(\eta_2, \eta_3)^2 d\eta_2 d\eta_3. \quad (17)$$

Accordingly, the variance $\sigma^2 u$ is given by

$$(\sigma^2 u)(x) = \sum_{j=1}^{\infty} \sum_{k=1}^{\infty} \lambda_j \lambda_k \psi_j(x) \psi_k(x) T_{jk}. \quad (18)$$

Proof. Due to the assumptions, L is self-adjoint. It is well-known that it then has a countably infinite discrete set of eigenvalues that we call $\{1/\lambda_n\}$ and the corresponding eigenfunctions $\{\psi_n\}$ are an orthonormal basis of $H_0^1(U)$; the minimum eigenvalue $1/\lambda_1$ is simple and has a positive eigenfunction [10, Theorems 8.37 and 8.38].

Regarding the Green's function G of L , the sets $\{\lambda_n\}$ and $\{\psi_n\}$ are the eigenvalues and eigenfunctions of G , i.e.,

$$\psi_n(x) = \lambda_n L \psi_n(x) \quad (19)$$

holds. Since $\{\psi_n\}$ is an orthonormal basis, the identity $f(x) = \sum_{n=1}^{\infty} \langle f, \psi_n \rangle \psi_n(x)$ holds and we can apply it to $f(x) := \delta(x - y)$ to find

$$LG(x, y) = \delta(x - y) = \sum_{n=1}^{\infty} \psi_n(x) \psi_n(y)$$

and therefore, using (19), we have

$$G(x, y) = \sum_{n=1}^{\infty} \lambda_n \psi_n(x) \psi_n(y).$$

Since the $\{\psi_n\}$ are orthonormal, the last equation yields

$$\langle G(x, \cdot), \psi_m \rangle = \int G(x, y) \psi_m(y) dy = \lambda_m \psi_m(x).$$

To solve equation (13) for the covariance, we consider the right-hand side

$$f(y, z) := \epsilon^4 \delta(y_1, z_1, y_2 - z_2, y_3 - z_3) \bar{R}(y_2, y_3)^2$$

and integrate it twice against the Green's function G of the operators L_y and L_z to find

$$\begin{aligned} (\text{cov } u)(y, z) &= \int_U \int_U f(\eta, \zeta) G(y, \eta) G(z, \zeta) d\eta d\zeta \\ &= \int_U \int_U f(\eta, \zeta) \sum_{j=1}^{\infty} \sum_{k=1}^{\infty} \lambda_j \psi_j(y) \psi_j(\eta) \lambda_k \psi_k(z) \psi_k(\zeta) d\eta d\zeta \\ &= \epsilon^4 \sum_{j=1}^{\infty} \sum_{k=1}^{\infty} \lambda_j \lambda_k \psi_j(y) \psi_k(z) T_{jk}, \end{aligned}$$

where the coefficients T_{jk} are defined in (17). This concludes the proof. \square

This proposition shows that the covariance and the variance can be approximated efficiently by taking a finite double sum in (16) using only the largest eigenvalues λ_j and λ_k . The details of such an algorithm are given in Appendix B. The quality of the approximation depends on the separation of the first N eigenvalues from the rest. A numerical example and a proposed improvement are discussed in §6.2 below.

6. Numerical verification. In order to verify the homogenization result in Theorem 8 and the spectral approximation in Proposition 16 numerically, two numerical calculations are presented here. Real-world calculations were presented in [11], where the models and equations of the present work were used to calculate electrostatic fluctuations in field-effect nanosensors.

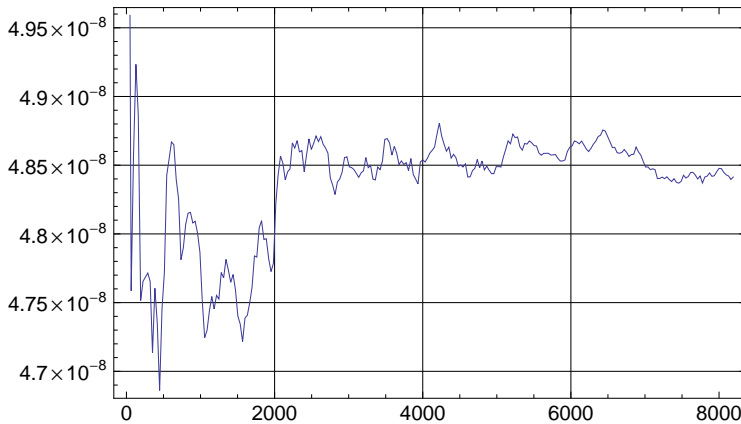


FIG. 2. The integral $\int_U \sigma^2 u dx$ of the variance as a function of the number of realizations in the case $K = 16^2$.

6.1. Numerical verification of the scaling law. For the numerical verification, we consider a three-dimensional example. We set $U := (0, 1)^3 \subset \mathbb{R}^3$, define $L := -\Delta$, and use an equidistant grid for the finite-difference discretization of L . For symmetry, the boundary layer is located at $x = 1/2$ so that the cells are

$$\mathcal{C}_k = \mathcal{C}_{(k_2, k_3)} = [\epsilon k_2, \epsilon(k_2 + 1)) \times [\epsilon k_3, \epsilon(k_3 + 1)).$$

The number of cells in each direction is always chosen as $k_2 = k_3$ and as a power of two; the height of the cells is chosen as ϵ in accordance with the multiscale ansatz (7), i.e., the volume of a single cell is always $1/\epsilon^3$. The boundary conditions are zero Dirichlet boundary conditions at $x_1 = 0$ and $x_1 = 1$ and zero Neumann boundary conditions at $x_2 = 0$, $x_2 = 1$, $x_3 = 0$, and $x_3 = 1$.

The charge concentrations $\rho(x, \omega)$ are constant and uniformly distributed in the interval $[0, 1]$ in each cell of the boundary layer; outside of the boundary layer, the charge concentration vanishes. The numerical verification for a large number of cells in the boundary layer is hampered by the fact that the direct or Monte-Carlo calculation of the variance requires many solutions of $Lu(x, \omega) = \rho(x, \omega)$ for randomly chosen ω . Calculations for total numbers of cells $K \in \{2^2, 4^2, 8^2, 16^2\}$ were performed with a grid size of $1/16$ in the finite-difference approximation. To calculate the variance, 8192 realizations were used in all four cases.

To verify that the number of realizations is sufficient for the calculation of the variance, the integral of the variance over the domain U is shown as a function of the number of realizations in Fig. 2 for the case $K = 16^2$. Fig. 3 shows plots of the variances for $K \in \{2^2, 4^2, 8^2, 16^2\}$ after 8192 realizations as the cell size is halved.

The results of the numerical calculations for the parameters described above are summarized in Table 1. As the number of cells in each direction is doubled in every refinement step, i.e., ϵ is halved, the scaling factor for the variance is given by Corollary 10 as $1/16$. The numerically approximated values of 7.8, 13.3, and 14.0 in Table 1 agree well with the theoretical value even for these small numbers of cells. The computational requirements for larger numbers of cells would be enormous due to

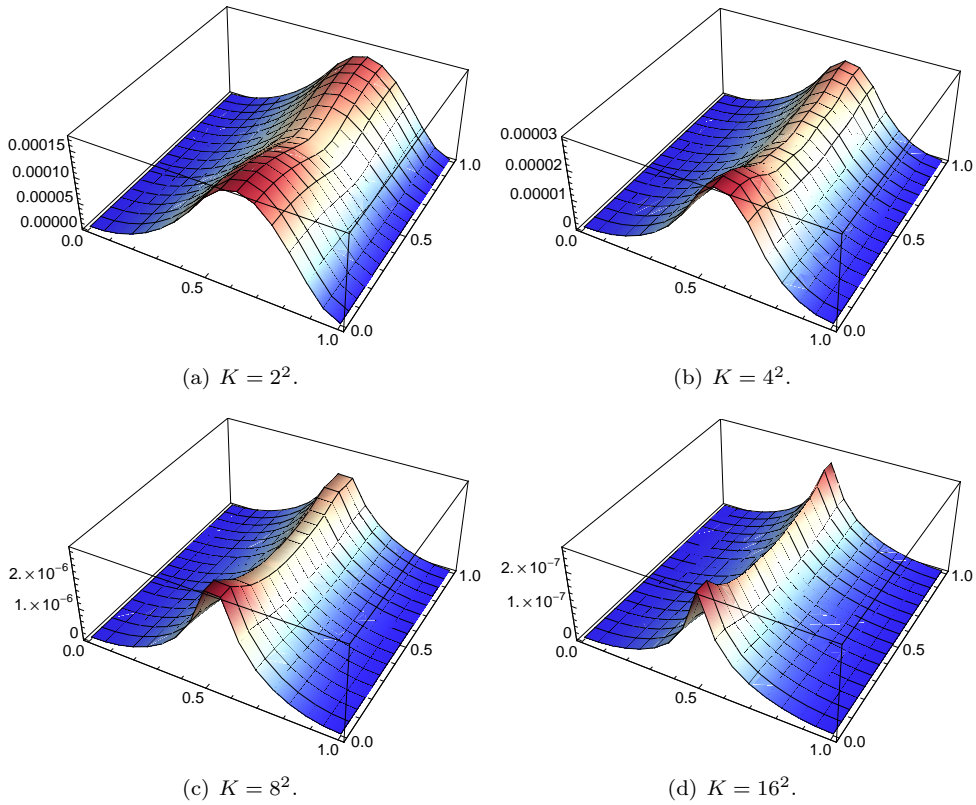


FIG. 3. The variances after 8192 realizations for the four cases $K \in \{2^2, 4^2, 8^2, 16^2\}$. The plots are two-dimensional ones for $z = 1/2$.

the stochastic nature of the problem, which underlines the importance of Corollary 9 and the scaling law in Corollary 10.

6.2. Numerical results for the spectral approximation. We continue to consider the Laplace operator and we define the domain to be $U := (-1/2, 1/2) \times (0, 1)^2 \subset \mathbb{R}^3$. The numerical grid is equidistant with m interior grid points and zero Dirichlet boundary conditions on ∂U . Therefore the eigensystem of the discretization has size m^3 and the eigenvalues are given by $(i^2 + j^2 + k^2)\pi^2$ with $i, j, k \in \{1, \dots, m\}$. We denote these eigenvalues by λ_μ with $\mu \in \{1, \dots, m^3\}$ so that $\lambda_1 \geq \dots \geq \lambda_{m^3}$. Due to the distribution of the eigenvalues, the spectral approximation grows slowly and usage of nearly the full spectrum in the approximation is necessary to achieve a good approximation; this is observed in Fig. 4, where the results for $m = 9$ are shown.

Therefore we propose to improve the approximation by a geometric factor. In view of (16), we define the geometric factor as

$$\gamma_{m,N} := \left(\frac{\sum_{\mu=1}^N \sum_{\nu=1}^N \lambda_\mu^2 \lambda_\nu^2}{\sum_{\mu=1}^{m^3} \sum_{\nu=1}^{m^3} \lambda_\mu^2 \lambda_\nu^2} \right)^{1/2} \approx \frac{\|\sigma^2 u_N\|_2}{\|\sigma^2 u\|_2},$$

where $\sigma^2 u_N$ denotes the truncated double sum defined in (20b). In the double sum, the largest N eigenvalues are used. Therefore the factor $\gamma_{m,N}$ represents a correction for

ϵ	number of cells in boundary layer	integral of variance	scaling factor for variance
1/2	$K = 2^2$	$\int \sigma^2 u = 7.0553 \cdot 10^{-5}$	
			7.8
1/4	$K = 4^2$	$\int \sigma^2 u = 9.0360 \cdot 10^{-6}$	
			13.3
1/8	$K = 8^2$	$\int \sigma^2 u = 6.7742 \cdot 10^{-7}$	
			14.0
1/16	$K = 16^2$	$\int \sigma^2 u = 4.8414 \cdot 10^{-8}$	

TABLE 1

Overview of the factors in the numerical verification. The predicted scaling factor for the variance is 16.

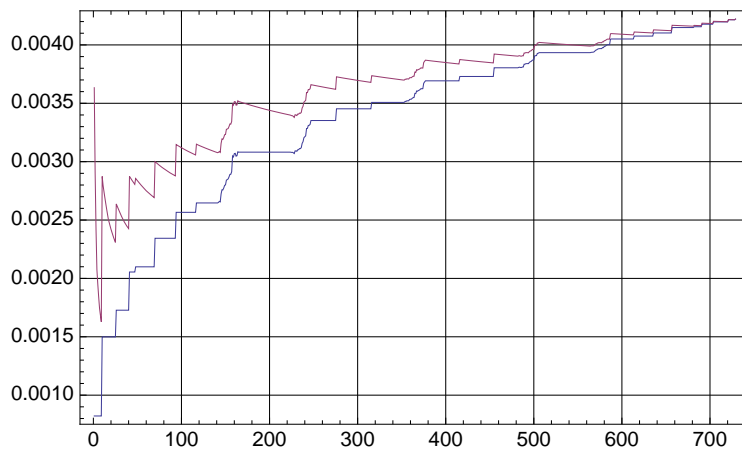


FIG. 4. The spectral approximation $\sigma^2 u_N(0, 1/2, 1/2)$ (lower line) and the corrected approximation $\sigma^2 u_N / \gamma_{m,N}(0, 1/2, 1/2)$ (upper line) as a function of N for the case $m = 9$.

the L^2 -norm of the variance taking into account the (in this case) known distribution of the eigenvalues. The improvement is shown in Fig. 4, where $\sigma^2 u_N$ and $\sigma^2 u_N / \gamma_{m,N}$ at the middle point of the domain are shown as functions of N , the number of eigenvalues used in the approximation.

7. Conclusion. In this work we treated the homogenization of boundary layers in stochastic elliptic partial differential equations. The results are limiting problems for the covariance and variance of the solution of the stochastic equation. From the limiting problems we deduced scaling laws for the covariance and variance. Also for the limiting problems, existence and uniqueness results and a priori bounds were given, as well as results for definiteness and symmetry. Finally, numerical results for the scaling law and a spectral approximation with a proposed correction factor were presented. Applications of this work include the simulation of electrostatics in nanotechnological devices such as field-effect sensors.

8. Acknowledgment. The first author acknowledges discussions with Robert W. Dutton and Yang Liu.

Appendix A. Proof of Lemma 11.

We first prove that $\|Lu\|_{L^2(U)}$ is indeed a norm. We denote the bilinear form associated with L by $a_1(u, v)$. Due to the assumptions, a_1 is continuous.

To see that a_1 is coercive, we note the estimate

$$\begin{aligned} a_1(u, u) &\geq \theta \|\nabla u\|_{L^2(U)}^2 - \|b\|_{L^\infty(U)} (\epsilon \|u\|_{L^2(U)}^2 + \delta \|\nabla u\|_{L^2(U)}^2) + \left(\inf_{x \in U} c\right) \|u\|_{L^2(U)}^2 \\ &= (\theta - \delta \|b\|_{L^\infty(U)}) \|\nabla u\|_{L^2(U)}^2 + \left(\inf_{x \in U} c - \epsilon \|b\|_{L^\infty(U)}\right) \|u\|_{L^2(U)}^2 \end{aligned}$$

with $\delta\epsilon = 1/4$. If $b = 0$ and $c \geq 0$, the Poincaré inequality $\|u\|_{L^2(U)} \leq C \|\nabla u\|_{L^2(U)}$ for $u \in H_0^1(U)$ establishes that a_1 is coercive. In the second case, i.e., if $\|b\|_{L^\infty}^2 \leq 4\theta \inf_{x \in U} c$, we set $\epsilon := (\inf_{x \in U} c) / \|b\|_{L^\infty(U)}$ so that the coefficient of $\|u\|_{L^2(U)}^2$ vanishes. Then $\delta = \|b\|_{L^\infty(U)} / (4 \inf_{x \in U} c)$, the coefficient of $\|\nabla u\|_{L^2(U)}^2$ is positive, and a_1 is again coercive.

Having established the existence and uniqueness of the solution, we note that $\|Lu\|_{L^2(U)} = 0$ implies $u = 0$ a.e. Therefore $\|Lu\|_{L^2(U)}$ is a norm.

We now show that the two norms are equivalent. First, we show that there is a constant C so that $\|Lu\|_{L^2(U)} \leq C \|u\|_{H^2(U)}$. Using Hölder's inequality for sums, we find

$$\begin{aligned} |Lu| &\leq \|A\|_{L^\infty(U)} \sum_{i,j=1}^d |u_{x_i x_j}| + \|b\|_{L^\infty(U)} \sum_{i=1}^d |u_{x_i}| + \|c\|_{L^\infty(U)} |u| \\ &\leq C \left(\sum_{i,j=1}^d |u_{x_i x_j}|^2 + \sum_{i=1}^d |u_{x_i}| + |u|^2 \right)^{1/2} \end{aligned}$$

and hence

$$\|Lu\|_{L^2(U)}^2 \leq C \|u\|_{H^2(U)}^2.$$

Second, we show that there is a constant C so that $\|u\|_{H^2(U)} \leq C \|Lu\|_{L^2(U)}$. This follows from the regularity result

$$\|u\|_{H^2(U)} \leq C \|f\|_{L^2(U)} \quad \forall u \in H^2(U) \cap H_0^1(U).$$

for elliptic equations $Lu = f$ with unique solutions (see, e.g., [9, Section 6.3]). \square

Appendix B. Algorithm for the spectral approximation.

The procedure based on Proposition 16 that was used in the calculations in §6.2 is described here.

(i) Given the boundary-value problem (1), let $\mathbf{u}, \mathbf{f} \in \mathbb{R}^M$ and $\mathbf{L} \in \mathbb{R}^{M \times M}$ be discretizations for the solution u , the inhomogeneity f , and the differential operator L . Then the discretization of the Green's function G is given by $\mathbf{G} = \mathbf{L}^{-1}$, since $\mathbf{u} = \mathbf{L}^{-1} \mathbf{f} = \mathbf{G} \sum_j \mathbf{f}_j \mathbf{e}_j = \sum_j \mathbf{f}_j \mathbf{G}_{\cdot, j} \approx \int f(y) G(x, y) dy = u(x)$. Since it is too computationally expensive to compute the Green's function $\mathbf{G} = \mathbf{L}^{-1}$, only the first $N \in \mathbb{N}$ eigenvalues and eigenfunctions are used. This yields the approximation

$$G(x, y) = \sum_{\nu=1}^{\infty} \lambda_\nu \psi_\nu(x) \psi_\nu(y) \approx \sum_{\nu=1}^N \lambda_\nu \psi_\nu(x) \psi_\nu(y) \approx \sum_{\nu=1}^N \lambda_\nu \mathbf{v}_i^\nu \mathbf{v}_j^\nu = \mathbf{G}_{ij},$$

where $\lambda_1 \geq \dots \geq \lambda_N$ holds for the eigenvalues λ_ν and eigenvectors \mathbf{v}^ν of \mathbf{G} for all $\nu \in \{1, \dots, N\}$. Here the index i in \mathbf{v}_i^ν denotes the component of the vector \mathbf{v}^ν that corresponds to the point x after discretization.

(ii) Compute the largest N eigenvalues λ_ν and their eigenvectors \mathbf{v}^ν of \mathbf{G} . These are smallest N eigenvalues and their eigenvectors of the known matrix \mathbf{L} .

(iii) Compute $T_{\mu\nu}$ for $\mu, \nu \in \{1, \dots, N\}$ in (17) by evaluating N^2 two-dimensional integrals. This yields

$$T_{\mu\nu} \approx \epsilon^4 \int_0^{L_3} \int_0^{L_2} \mathbf{v}^\mu(0, \eta_2, \eta_3) \mathbf{v}^\nu(0, \eta_2, \eta_3) \bar{R}(\eta_2, \eta_3)^2 d\eta_2 d\eta_3.$$

(iv) Compute the covariance or the variance by summing the N^2 terms in (16). The approximations are given by

$$(\text{cov } u)(y, z) \approx \sum_{\mu=1}^N \sum_{\nu=1}^N \lambda_\mu \lambda_\nu \mathbf{v}^\nu(y) \mathbf{v}^\mu(z) T_{\mu\nu}, \quad (20a)$$

$$(\sigma^2 u)(x) \approx \sigma^2 u_N(x) := \sum_{\mu=1}^N \sum_{\nu=1}^N \lambda_\mu \lambda_\nu \mathbf{v}^\nu(x) \mathbf{v}^\mu(x) T_{\mu\nu}. \quad (20b)$$

REFERENCES

- [1] G. ALLAIRE, *Homogenization and two-scale convergence*, SIAM J. Math. Anal., 23 (1992), pp. 1482–1518.
- [2] G. ALLAIRE, C. CONCA, AND M. VANNINATHAN, *Spectral asymptotics of the Helmholtz model in fluid-solid structures*, Internat. J. Numer. Methods Engrg., 46 (1999), pp. 1463–1504.
- [3] I. BABUŠKA AND P. CHATZIPANTELIDIS, *On solving elliptic stochastic partial differential equations*, Comput. Methods Appl. Mech. Engrg., 191 (2002), pp. 4093–4122.
- [4] I. BABUŠKA, F. NOBILE, AND R. TEMPONE, *A stochastic collocation method for elliptic partial differential equations with random input data*, SIAM Rev., 52 (2010), pp. 317–355.
- [5] I. BABUŠKA, R. TEMPONE, AND G. ZOURARIS, *Galerkin finite element approximations of stochastic elliptic partial differential equations*, SIAM J. Numer. Anal., 42 (2004), pp. 800–825.
- [6] ———, *Solving elliptic boundary value problems with uncertain coefficients by the finite element method: the stochastic formulation*, Comput. Methods Appl. Mech. Engrg., 194 (2005), pp. 1251–1294.
- [7] A. BULYHA, C. HEITZINGER, AND N. MAUSER, *An algorithm for three-dimensional Monte-Carlo simulation of biofunctionalized boundary layers*, (2010). *Submitted for publication*.
- [8] M. DEB, I. BABUŠKA, AND J. ODEN, *Solution of stochastic partial differential equations using Galerkin finite element techniques*, Comput. Methods Appl. Mech. Engrg., 190 (2001), pp. 6359–6372.
- [9] L. EVANS, *Partial Differential Equations*, American Mathematical Society, 1998.
- [10] D. GILBARG AND N. TRUDINGER, *Elliptic Partial Differential Equations of Second Order*, Springer-Verlag, 2001.
- [11] C. HEITZINGER, Y. LIU, N. J. MAUSER, C. RINGHOFER, AND R. W. DUTTON, *Calculation of fluctuations in boundary layers of nanowire field-effect biosensors*, J. Comput. Theor. Nanosci., 7 (2010). *In print*.
- [12] C. HEITZINGER, N. MAUSER, AND C. RINGHOFER, *Multiscale modeling of planar and nanowire field-effect biosensors*, SIAM J. Appl. Math., 70 (2010), p. 1634–1654.
- [13] H. HOLDEN, B. ØKSENDAL, J. UBØE, AND T. ZHANG, *Stochastic Partial Differential Equations*, Springer-Verlag, New York, Dordrecht, Heidelberg, London, 2nd ed., 2010.
- [14] A. JENTZEN AND P. KLOEDEN, *The numerical approximation of stochastic partial differential equations*, Milan J. Math., 77 (2009), pp. 205–244.
- [15] A. KEESE, *A review of recent developments in the numerical solution of stochastic partial differential equations (stochastic finite elements)*, Informatikbericht 2003-06, Institute of Scientific Computing, Technical University Braunschweig, Brunswick, Germany, Oct. 2003.

- [16] A. KÖCK, A. TISCHNER, T. MAIER, M. KAST, C. EDTMAIER, C. GSPAN, AND G. KOTHEITNER, *Atmospheric pressure fabrication of SnO₂-nanowires for highly sensitive CO and CH₄ detection*, Sensors and Actuators B, 138 (2009), pp. 160–167.
- [17] H. MATTHIES AND A. KEESE, *Galerkin methods for linear and nonlinear elliptic stochastic partial differential equations*, Comput. Methods Appl. Mech. Engrg., 194 (2005), pp. 1295–1331.
- [18] G. PAVLIOTIS AND A. STUART, *Multiscale Methods: Averaging and Homogenization*, Springer-Verlag, Berlin, 2007.
- [19] E. STERN, J. KLEMIC, D. ROUTENBERG, P. WYREMBAK, D. TURNER-EVANS, A. HAMILTON, D. LAVAN, T. FAHMY, AND M. REED, *Label-free immunodetection with CMOS-compatible semiconducting nanowires*, Nature, 445 (2007), pp. 519–522.
- [20] E. STERN, A. VACIC, N. RAJAN, J. CRISCIONE, J. PARK, B. ILIC, D. MOONEY, M. REED, AND T. FAHMY, *Label-free biomarker detection from whole blood*, Nature Nanotechnology, 5 (2010), pp. 138–142.
- [21] B. TIAN, T. COHEN-KARNI, Q. QING, X. DUAN, P. XIE, AND C. M. LIEBER, *Three-dimensional, flexible nanoscale field-effect transistors as localized bioprobes*, Science, 329 (2010), pp. 830–834.
- [22] A. TISCHNER, T. MAIER, C. STEPPER, AND A. KÖCK, *Ultrathin SnO₂ gas sensors fabricated by spray pyrolysis for the detection of humidity and carbon monoxide*, Sensors and Actuators B, 134 (2008), pp. 796–802.
- [23] X. WAN, B. ROZOVSKII, AND G. KARNIADAKIS, *A stochastic modeling methodology based on weighted Wiener chaos and Malliavin calculus*, Proc. Nat. Acad. Sci. U.S.A., 106 (2009), pp. 14189–14194.
- [24] G. ZHENG, F. PATOLSKY, Y. CUI, W. U. WANG, AND C. M. LIEBER, *Multiplexed electrical detection of cancer markers with nanowire sensor arrays*, Nature Biotechnology, 23 (2005), pp. 1294–1301.